Bull. Spec. Astrophys. Obs., 2000, 50, 60–69

The primary component of υ Sagittarius is a neon star

V.V. Leushin

Special Astrophysical Observatory of the Russian AS, Nizhnij Arkhyz 369167, Russia

Received February 23, 2000; accepted November 4, 2000.

Abstract. From photographic and CCD spectra the abundance of neon and other elements in the atmosphere of the υ Sgr primary component has been derived. The values of T_{eff} = 13500 ± 150 K and log g = 2.0 ± 0.5 obtained earlier have been confirmed; the value of the turbulent velocity in the region of neon line formation, V_t(Ne) = 12 km/s, has been found; the abundances of light elements H — 10^{-4}, He — 0.93, C — 0.014, N — 0.023, and O — 0.002 in mass have been refined. A great overabundance of neon has been found, its abundance with a high accuracy is log(N(Ne)/ΣN$_i$) = −2.76 ± 0.16 (about 1 % in mass).

Key words: stars: abundances — stars: binaries — stars: individual: υ Sagittarius

1. Introduction

The unique chemical composition of the bright component of the helium binary system υ Sgr is associated with its evolutionary status and some individual characteristic properties of the star's history. The observed proportion of hydrogen, helium and CNO group elements was discussed in detail in our previous papers (Leushin, Topilskaya, 1987; Leushin et al., 1998) and is quantitatively explained by assuming the main component of υ Sgr to be a product of evolution of a star with a mass of 7 $M_\odot$. The duration of its evolution from the main sequence is approximately $6 \cdot 10^7$ years. About $5 \cdot 10^6$ years ago, when at the centre of the star the helium-to-carbon conversion was in progress, at the boundary of the helium core a layer source of hydrogen burning generated. As a result, the star lost almost the whole hydrogen envelope.

The processes of light mixing triggered at that moment created the observed abundances of H, He, C, N and O in the atmosphere of the system's bright component (Leushin et al., 1998). This kind of processes are possible in the majority of stars that have reached the stage of helium depletion. However, an indispensable condition for chemical composition anomalies on the surface like those in υ Sgr to arise is the process of losing the envelopes (hydrogen and helium) exactly in multiple stellar systems. The gravitational interaction between the components in such systems may stimulate mixing of matter in zones with different chemical composition and nuclear processes. The latter is a necessary condition for the appearance of the observed anomalies.

Variations of intensity and duration of mixing and its effects at different stages of nuclear evolution may change essentially the final chemical composition of the atmospheres of helium stars. Thus, evolution and gravitational effects may cause the chemical composition of helium stars to be rather diversified, which is actually observed.

In connection with the above-said the distinctions in chemical composition of helium stars, members of multiple systems (binaries, as a rule), are defined by basic parameters (mass and radius of the components, distribution of mass along the radius, original chemical composition) and by evolution history of a system (duration of evolution, degree of interaction of the components, size and eccentricity of orbits, etc.). Thus, each of the characteristic properties of chemical composition of helium stars may be rigidly determined by physical properties of a system.

Taking into account all stated above, we calculated the history of chemical evolution of υ Sgr (Leushin et al., 1997) which explains the observed abundances of hydrogen, helium and CNO group elements. Light elements from hydrogen to oxygen were involved in the computation since it was assumed that the nuclear evolution of matter of the main component of υ Sgr terminated by helium depletion. The estimate of neon abundance that we have obtained (about 9% in mass) demanded more advanced stages of nuclear evolution. However, this estimate is uncertain since it has been made from blue region spectra, where neon lines are very few.

The aim of the present paper is to evaluate the neon abundance in the atmosphere of the main component of υ Sgr on the basis of spectral data obtained in the red spectral region, where neon lines are quite numerous.

Table 1: *Spectral data for analysis of υ Sgr*

Date	No. of the spectrum	Detector	Spectrum region	Resolution	S/N ratio	Dispersion
17.05.78	1,2	Kodak103aO	3900 – 5000	10000	≅40	8 Å/mm
14.06.78	33-35	Kodak103aO	3900 – 5000	10000	≅40	8 Å/mm
13.08.86	21	Kodak103aO	3900 – 5000	40000	≅40	1.8 Å/mm
15.06.96	c11604s	CCD 1242×1192 Wight Instr.(GB)	3400 – 10000	40000	≅200	0.18 Å/pic.

2. Observations

For analysis of the main component of υ Sgr we used spectrograms taken with the SAO RAS 6 m telescope Main Stellar Spectrograph on emulsions Kodak 103aO and Kodak OaO with dispersions of 2–8 Å/mm in H_γ from 1976 to 1986, and the spectra obtained with the echelle spectrograph of the 1 m telescope of SAO RAS (Musaev, 1993) using a CCD matrix.

Relevant data are collected in Table 1.

The absorption lines in the spectra of the υ Sgr bright component that we have identified and measured from the photographic spectra in the region $\lambda\lambda$ 3800–4680 ÅÅ are given in the paper by Kravtsov, Leushin (1981). The results for the lines NeI measured in the region $\lambda\lambda$ 5400–8500 ÅÅ from CCD spectra are listed in Table 2. The table presents atomic parameters, equivalent widths and values of neon abundance obtained from corresponding lines. The abundance value is given in $\log(N(Ne)/\Sigma N_i)$. Since the spectrum of the υ Sgr main component is rich in spectral lines, there are practically no lineless regions in the continuous spectrum. The latter condition leads to the fact that even with a signal-to-noise ratio of ≅ 200 the accuracy of the equivalent width values cannot be better than 10 %.

To analyse the neon lines in the spectrum of υ Sgr, we have employed the $\log gf$ values from Kasabov and Eliseev (1973) and also a compilation of $\log gf$ data in the VALD system (Ryabchikova et al., 1999). Table 2 tabulates the latter. A comparison of oscillator strengths from these papers is shown in Fig.1 and points to a good enough fit between them:

$$\log gf(\mathrm{VALD}) = 0.98 \times \log gf(\mathrm{KE}) + 0.07.$$

It should nevertheless be noted that there are some discrepancies in $\log gf$ values for some lines.

3. Model atmosphere of the bright component of υ Sgr

The used procedure of the atmosphere chemical composition analysis is described by Leushin (1995). The model atmosphere was chosen earlier (Leushin, Topilskaya, 1985). The basic parameters of the computed model (T_e = 13500 K, $\log g$ = 2.0, abundances of hydrogen, helium, carbon, nitrogen, and oxygen are 10^{-4}, 0.93, 0.013, 0.042 and 0.008, respectively) were confirmed in later studies (Leushin et al., 1997).

Nevertheless, the new data, obtained from better spectra with an essentially higher resolution necessitated some revision when computing the model atmosphere of υ Sgr. In particular we had to take more precise account of the influence of the atmosphere chemical composition anomalies of the star under study as compared to the standard (solar) anomalies and backwarming. The original chemical abundance of the model atmosphere varied within ±0.6 dex from those presented above. The abundance of the rest of the elements was taken by +0.3 dex higher than the solar one. The model was computed by the programme SAM1, which we adapted for the input data to be used in the programme KONTUR (Leushin, Topilskaya, 1986).

Calculations of models with different proportions of hydrogen, helium, elements of CNO group and neon in the mentioned above limits as compared to those determined earlier (Leushin, Topilskaya, 1987) do not practically change the structure of the model atmosphere. For this reason, the model atmosphere variations were not included in the iteration process of determining neon abundance in υ Sgr.

The employed model atmosphere is planeparallel, which is not crucial in our analysis. Calculations show that the linear depth of the atmosphere H (up to τ=1.0) is ≅ 10^6 km. Thus, for υ Sgr H/R≅ 0.04 the atmosphere may be considered planeparallel.

4. Turbulent velocity from neon lines

The turbulent velocity value V_t in the atmosphere of υ Sgr, found by Kravtsov, Leushin (1981) and Leushin, Topilskaya (1987) from FeI, FeII, CrII, and TiII lines in the blue region of the spectrum, varies from 5 to 10 km/s. Our spectral data made it possible to determine the turbulent velocity in the atmosphere of υ Sgr from NeI lines in the red region of the spectrum. With this purpose we made a series of calculations of theoretical curves of growth for 40 NeI lines with the programme KONTUR (Leushin,

Table 2: *Parameters, equivalent widths* (W_λ, *mÅ) and neon abundance values*

λ,Å	ε_i, eV	log gf	W_λ	log N(Ne)/Σ N_i
5433.65	18.38	-2.17	28.0	-2.65
5448.51	18.38	-3.35	5.0	-2.34
5852.49	16.65	-0.46	390.0	-2.61
5881.90	16.62	-0.67	295.0	-2.96
5944.83	16.62	-0.12	495.0	-2.35
5974.63	18.64	-0.71	200.0	-2.59
5975.53	16.62	-1.26	198.0	-2.96
6029.99	16.67	-1.04	258.0	-2.78
6046.14	18.61	-2.19	15.0	-2.73
6074.34	16.67	-0.47	325.0	-2.96
6096.16	16.67	-0.27	415.0	-2.65
6118.03	18.63	-1.82	60.0	-2.51
6128.45	16.67	-1.94	160.0	-2.44
6143.06	16.62	-0.10	400.0	-2.92
6163.59	16.72	-0.59	390.0	-2.45
6217.28	16.62	-1.14	240.0	-2.80
6266.49	16.71	-0.53	339.0	-2.85
6293.74	18.69	-1.77	51.0	-2.59
6304.79	16.67	-1.41	170.0	-2.93
6313.69	18.69	-1.91	17.0	-2.98
6328.16	18.70	-1.04	140.0	-2.58
6334.43	16.62	-0.31	363.0	-2.92
6351.86	18.71	-2.04	27.0	-2.64
6382.99	16.67	-0.26	390.0	-2.79
6402.25	16.62	0.36	550.0	-2.59
6421.71	18.72	-1.97	16.0	-2.89
6506.53	16.67	0.03	417.0	-2.94
6532.88	16.67	-0.70	255.0	-3.10
6598.95	16.85	-0.35	402.0	-2.56
6602.91	18.69	-1.76	51.0	-2.93
6678.28	16.85	-0.11	350.0	-3.10
6678.33	18.70	-1.53	50.0	-2.74
6717.04	16.85	-0.31	320.0	-3.06
6929.47	16.85	0.03	450.0	-2.69
7032.41	16.62	-0.25	450.0	-2.52
7173.94	16.85	-1.31	150.0	-3.06
7245.17	16.67	-0.60	350.0	-2.68
7304.82	18.96	-2.17	7.0	-2.80
7438.90	16.71	-1.15	270.0	-2.55
7488.87	18.38	0.05	334.0	-2.64

Topilskaya, 1986) for the model atmosphere with parameters T_{eff} = 13500 K, and log g = 2.0 and turbulent velocity from 7.5 km/s to 15 km/s. From the curves of growth and measured values of equivalent widths we estimated neon abundance from the number of atoms — log (N(Ne)/ΣN$_i$) for each value of turbulent velocity. The observed equivalent widths were compared with the theoretical ones for abundances obtained with different values of turbulent velocity. Fig. 2 shows neon abundance variations as a function of equivalent width for two values V_t=7.5 km/s and V_t=12.0 km/s. Table 3 gives the values of the coefficients of linear regressions for the relation mentioned

$$\log (N(Ne)/\Sigma N_i) = \log (N(Ne)/\Sigma N_i)_0 + k \times W_\lambda,$$

log (N(Ne)/ΣN$_i$)$_0$ is the value in ordinate axis at zero value of the abscissa axis.

From Fig. 2 it is seen that for V_t = 7.5 km the value log(N(Ne)/ΣN$_i$), obtained from the equivalent width, increases with equivalent width. This increase is caused by underestimation of the turbulent velocity at calculation of a theoretical curve of growth. If the value of the turbulent velocity in theoretical calculations is chosen correctly, the element abundances obtained are not caused by the value of the line equivalent widths. Thus, the correct value of V_t can be determined from the change of the sign of the linear regression coefficient in the ratio log (N(Ne)/ΣN$_i$) = log (N(Ne)/ΣN$_i$)$_0$ + k × W_λ. As is seen from the table, V_t = 12.0 km/s meets this condition. This is also confirmed by the root-mean-square error presented in the last column of the table, which decreases when approaching the correct value of V_t.

Formally V_t is determined here with an accuracy of ±0.1 km/s, however, it should be borne in mind that the real values of V_t in the atmosphere of υ Sgr vary undoubtedly over a rather wide range (apparently from 5 to 12 km/s), and since the spectral lines form in the whole depth of the atmosphere, we may speak only about an average value in the region of line formation.

On the other hand, the spectrum of υ Sgr reveals all the features of an envelope and expanding inhomogeneous atmosphere: non-symmetrical profiles of P Cyg type in some lines, and also a strong emission in H_α. The extent and non-stationarity of the atmosphere cause inhomogeneous motions in height. For determination of element abundances the values of turbulent velocity variations are of great importance. As it was mentioned earlier Kravtsov and Leushin (1981) the noted V_t variations lie within 5 to 10 km/s. A study of lines in the blue region gives a value close to 7.5 km/s, and in the red region close to 12 km/s. Neon lines that we have measured are in the red region of the spectrum and give exactly this value of turbulent velocity.

Because of low hydrogen abundance, the atmosphere of υ Sgr is rather transparent and ion lines with different ionization potentials form at different depths. The lines in red and blue spectrum regions form also at different depths. This fact causes a notable difference in turbulent velocity determined from these elements, if the turbulent velocity varies with depth. The difference in turbulent velocities determined from FeI, FeII, CrII, TiII and NeI lines is indicative of velocity variations with depth, which confirms our assumption on mixing of the zones with

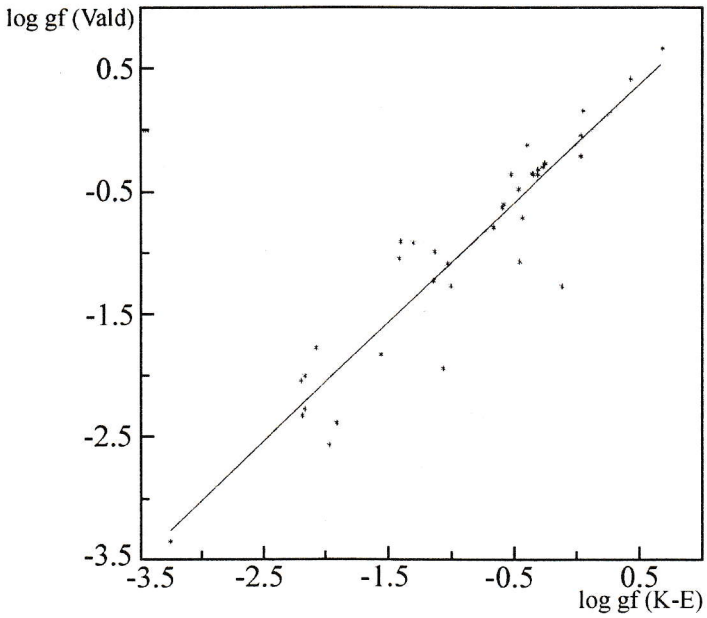

Figure 1: *A comparison of the oscillator strength values of NeI.*

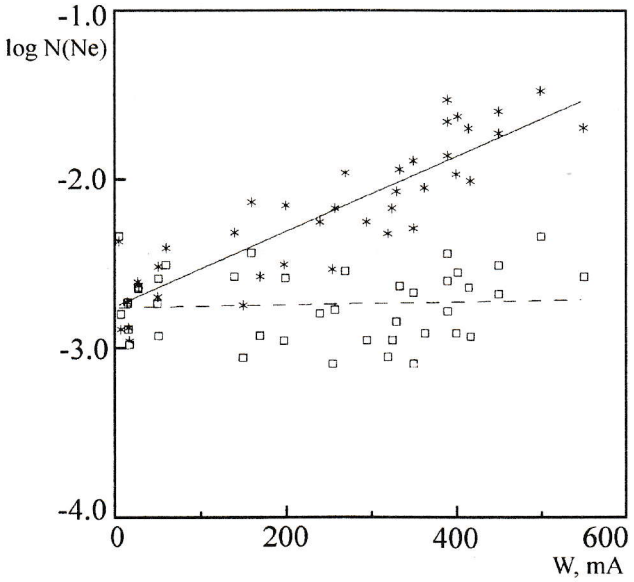

Figure 2: *Neon abundance as a function of* W_λ *for* $V_t = 7.5$ *km/s (asterisks) and* $V_t = 12.0$ *km/s (rectangles).*

different chemical composition (Leushin et al., 1998).

5. Neon abundance in the atmosphere of υ Sgr

Table 2 presents the equivalent widths of NeI lines and $\log(N(Ne)/\Sigma N_i)$ obtained with an average value of turbulent velocity, $V_t = 12.0$ km/s. The mean value of the neon abundance with the standard deviation from the average for all 40 lines is $\log(N(Ne)/\Sigma N_i) = -2.74 \pm 0.20$. The accuracy of determination of the element abundance from the line equivalent width depends on the accuracy of continuum level placement and measurement of the line contour. The problem of resolving element lines under study and placement of a continuous spectrum is not a trivial one for the spectra with strong blending. An analysis of abundance from the line contours with calculation of the regions of the synthetic spectrum can be made with more accurate allowance for blending and location of

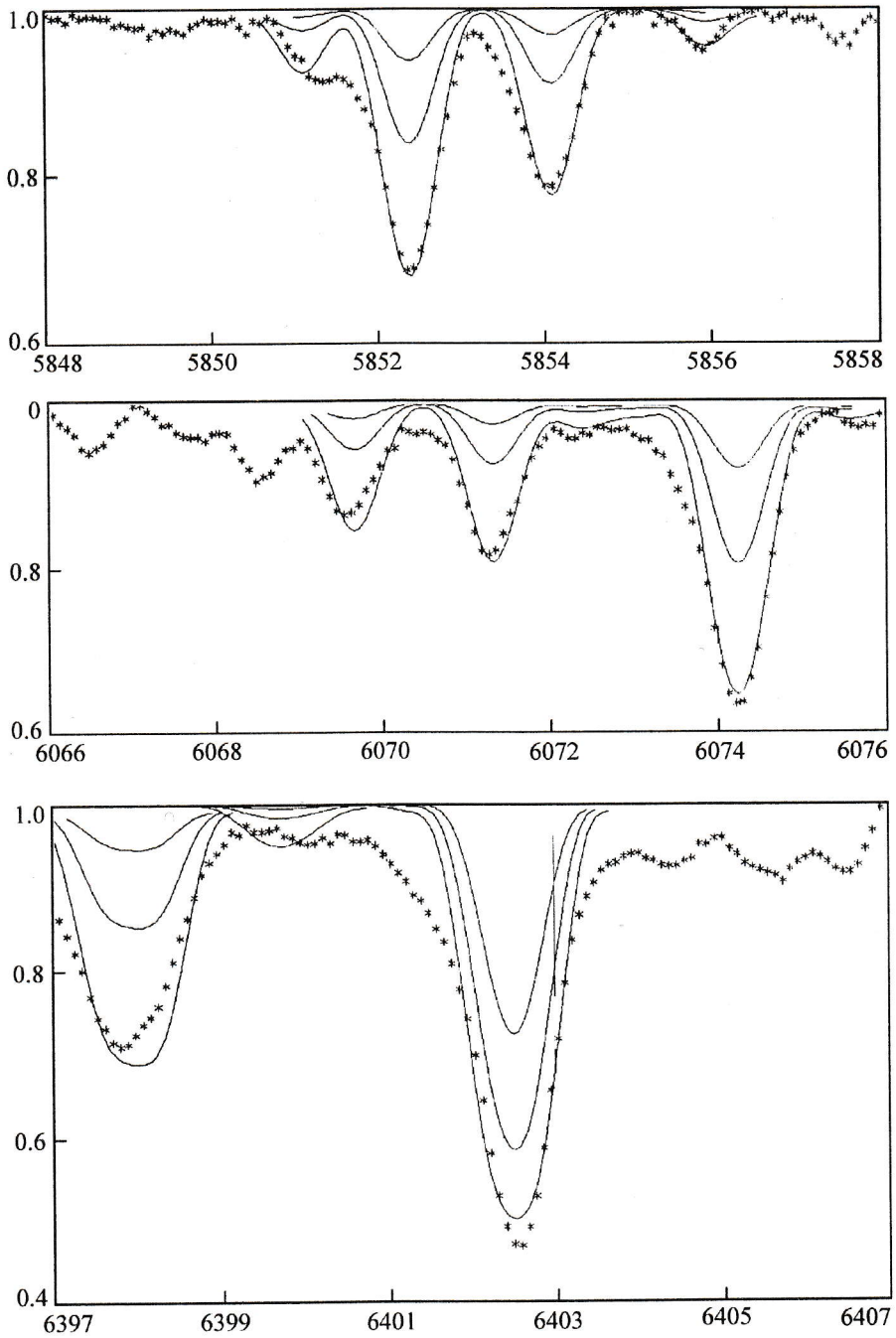

Figure 3: *Regions of synthetic spectra round NeI lines. Asterisks — the observed spectrum, lines — calculated spectrum with the element abundance variations by -0.5 and 1.0 dex relative to the data of Table 4.*

the continuous spectrum. The blending here is taken into account by including into the synthetic profile of all the lines falling within this spectral interval. At the same time, the procedure of calculation demands knowledge of the parameters of all lines of the blend, which cannot be always done especially for faint lines. Practically for all neon lines in the spectrum of υ Sgr unidentified components can be found. Besides, as compared with the equivalent width the line contours are strongly affected by the influence of dynamic parameters of the atmosphere envelope expansion and outflow, differential rotation of the atmosphere, meridional flows, variations of turbulent velocity with height, etc.). Nevertheless abundances

Table 3: *Coefficients of linear regressions for the relation of the calculated neon abundance and equivalent line width at different values of turbulent velocity; corresponding average values* $\log(N(Ne)/\Sigma N_i)$ *and the root-mean-square error of this average* ($\pm\Delta(\log N)$)

V_t km/s	$\log(N(Ne)/\Sigma N_i)_0$	k	$\log(N(Ne)/\Sigma N_i)$	$\Delta(\log N)$
15.0	-2.707	-0.00090	-2.929	±0.040
12.5	-2.732	-0.00018	-2.776	±0.033
12.0	-2.740	-0.000003	-2.740	±0.033
11.9	-2.740	+0.00003	-2.731	±0.033
11.8	-2.741	+0.00007	-2.722	±0.033
11.5	-2.745	+0.00010	-2.698	±0.033
10.0	-2.762	+0.00086	-2.552	±0.039
7.5	-2.756	+0.00220	-2.216	±0.064

are determined more reliably from the contours than from the net line intensities.

To specify the neon abundance, a calculation of the synthetic spectra around the NeI line was made. Table 4 presents the lists of spectral lines with atomic parameters for the regions of the synthetic spectrum in which NeI lines are located. The synthetic spectrum for each of these regions of the spectrum was computed with different values of element abundances. The last column of Table 4 shows the abundances of $\log(N_k/\Sigma N_i)$ for each of the elements, at which the theoretically computed spectrum describes best the observations. Fig. 3 shows the corresponding regions of the synthetic and observed spectra. The differences between the theoretical curves are due to the reduction of the element abundances (with respect to that given in Table 4) by -0.5 and -1.0 dex in the number of atoms.

Below are presented some considerations on the comparison of the synthetic and observed spectra.

NeI λ 5852.49. The theoretical synthetic spectrum describes well the contour of the neon line and of the blend NI (λ 5854.05) and FeII (λ 5854.19). On the red side of the NeI line, there is an unidentified line λ 5851.6 Å with R≅ 0.09. The neon abundance: $\log(N(Ne)/\Sigma N_i) = -3.06$.

NeI λ 5944.83. A blend with the H_2O lines of the atmosphere.

NeI λ 6074.34. The synthetic spectrum describes well the observed one, however, in the blue wing of NeI the line λ 6073.2 with R≅ 0.08 is not identified. The neon abundance: $\log(N(Ne)/\Sigma N_i) = -3.01$.

NeI λ 6096.16. Coincidence of the theoretical and observed contours is good. The line component is visible on the red side of the neon line. Apparently, it is an unidentified line. The neon abundance: $\log(N(Ne)/\Sigma N_i) = -3.04$.

NeI λ 6143.06. Coincidence of the theoretical and observed contours is within the observation errors. The line component on the red side of the neon line can be described by increasing of $\log(N(Fe)/\Sigma N_i)$ for Ti and Fe by 0.6 dex in the calculation of TiII λ 6141.51 and FeII λ 6141.85 lines. The neon abundance value: $\log(N(Ne)/\Sigma N_i) = -2.76$. Incorrect placing of the continuous spectrum is possible.

NeI λ 6163.59. The neon abundance is determined within $-3.06 < \log(N(Ne)/\Sigma N_i) < -2.86$. The uncertainty is associated with the blend which is not resolved with NI λ 6163.21 line.

NeI λ 6266.50. The neon abundance is determined very reliably: $\log(N(Ne)/\Sigma N_i) = -2.74$.

NeI λ 6328.16 and λ 6334.43. The neon abundance is determined reliably: $\log(N(Ne)/\Sigma N_i) = -2.74$. In both neon lines asymmetry of the red wing is seen, which is determined in other lines as an unidentified blend.

NeI λ 6401.08 and λ 6402.25. NeI λ 6401.08 line gives an abundance $\log(N(Ne)/\Sigma N_i) = -2.66$ by 0.1 dex higher than the line λ 6402.25. Thus, we may expect here $\log(N(Ne)/\Sigma N_i) = -2.71$.

NeI λ 6506.30. The theoretical contour does not describe completely the line wings. Apparently there are unidentified lines: blue — λ 6506.0, R=0.05, red — λ 6507.8, R=0.09. The neon abundance: $\log(N(Ne)/\Sigma N_i) = -2.76$.

NeI λ 6532.88. The contour and vicinity of NeI line are strongly blended with H_2O lines of the atmosphere. However, the estimate of the neon abundance is reliable: $\log(N(Ne)/\Sigma N_i) = -3.04$.

NeI λ 6678.28. The neon abundance is determined from two blending lines NeI λ 6678.28 and λ 6678.33. The weighted mean abundance value: $\log(N(Ne)/\Sigma N_i) = -2.80$.

NeI λ 6929.47. The spectrum is overcrowded with H_2O lines of the atmosphere. Neon abundance estimate: $\log(N(Ne)/\Sigma N_i) = -2.66$.

NeI λ 7032.41. The theoretical and observed contours coincide. On the blue side of the neon line there is a strong unidentified blend λ 7031.2, R=0.18. The neon abundance: $\log(N(Ne)/\Sigma N_i) = -2.64$.

Table 4: *Line parameters for calculation of synthetic spectra*

λ,Å	Ion	ε eV	log gf	logN
5428.64	SI	13.58	-0.31	-3.94
5429.79	FeII	12.89	0.12	-3.90
5429.81	FeI	4.74	-0.98	-3.90
5429.82	FeII	10.60	0.46	-3.90
5431.54	FeII	8.34	-2.26	-3.90
5432.77	SII	13.62	-0.61	-3.94
5432.97	FeII	3.27	-3.63	-3.90
5433.66	NeI	18.38	-2.27	-2.74
5434.39	TiII	7.87	-4.16	-5.65
5445.81	FeII	10.54	-0.11	-3.90
5446.82	FeII	13.52	0.79	-3.90
5429.92	FeII	0.99	-1.58	-3.90
5448.51	NeI	18.38	-3.35	-2.84
5851.05	CI	8.77	-1.72	-1.72
5851.21	NiII	9.21	-2.28	-5.47
5851.40	VII	9.12	-1.51	-6.63
5852.49	NeI	16.85	-0.46	-3.06
5854.05	NI	11.84	-2.4	-2.19
5854.19	FeII	10.74	-0.19	-4.10
5854.27	VII	9.09	-0.27	-6.63
5854.30	CI	10.02	-3.74	-1.72
5854.45	FeII	11.09	-1.48	-4.10
5856.00	NI	11.84	-2.08	-2.19
5881.90	NeI	16.62	-0.67	-2.80
5944.83	NeI	16.62	-0.12	-2.50
5974.63	NeI	18.64	-0.71	-2.60
5975.53	NeI	16.62	-1.26	-2.82
6024.02	FeII	10.83	-0.48	-3.80
6024.05	FeI	4.55	-0.09	-3.80
6024.13	PII	10.76	0.18	-5.22
6029.87	SiI	5.98	-0.42	-4.16
6029.99	NeI	16.67	-1.08	-2.74
6031.79	FeII	7.71	-3.86	-3.90
6034.02	PII	10.74	-0.14	-5.72
6043.05	PII	10.80	0.40	-5.22
6045.22	TiII	8.08	-1.04	-5.65
6045.46	FeII	6.21	-2.61	-3.90
6045.82	FeII	10.71	-0.97	-3.90
6046.03	SI	7.87	-1.03	-3.94
6046.14	NeI	18.61	-2.32	-2.64

Table 4: *Line parameters for calculation of synthetic spectra (continued)*

λ,Å	Ion	ε eV	log gf	logN
6046.44	OI	10.99	-1.37	-3.26
6071.43	FeII	10.71	-0.19	-4.10
6071.87	FeII	10.84	-1.56	-4.10
6072.45	TiII	8.11	0.141	-5.65
6072.49	FeII	10.85	-1.11	-4.10
6073.76	TiII	8.10	-0.14	-5.65
6074.34	NeI	16.67	-0.47	-3.06
6075.80	NI	11.60	-2.12	-2.39
6091.07	FeII	10.85	-2.25	-4.20
6092.13	SII	14.16	-0.93	-4.94
6092.20	TiII	8.10	-2.00	-5.65
6092.83	CI	8.85	-3.17	-2.02
6094.29	CI	8.85	-3.75	-2.02
6095.56	TiII	8.12	-2.16	-5.65
6095.78	NI	12.13	-2.14	-1.89
6095.79	NI	12.12	-2.92	-1.89
6095.89	FeII	10.75	-1.92	-4.10
6096.16	NeI	16.67	-0.27	-3.06
6096.32	FeII	11.21	-0.84	-4.10
6118.03	NeI	18.63	-1.82	-2.55
6128.45	NeI	16.67	-1.94	-2.65
6138.02	FeII	10.74	-1.21	-3.9
6138.94	SII	17.40	-0.90	-3.94
6141.52	TiII	8.12	-0.32	-5.05
6141.85	FeII	11.27	-0.87	-3.9
6142.51	NeI	18.69	-1.40	-2.76
6142.70	NI	11.60	-3.19	-1.89
6143.06	NeI	16.62	-0.35	-2.76
6144.96	CaII	9.24	-1.20	-4.52
6145.02	SiI	5.62	-0.82	-3.60
6158.15	OI	10.74	-1.89	-3.46
6158.17	OI	10.74	-1.03	-3.46
6158.19	OI	10.74	-0.44	-3.46
6159.70	TIII	8.11	-1.15	-5.65
6159.71	TiII	8.11	-2.82	-5.65
6160.51	FeII	11.24	-1.11	-3.90
6161.03	CrII	11.04	0.573	-4.86
6163.21	NI	12.12	-3.23	-2.39
6163.59	NeI	16.72	-0.59	-3.06
6164.66	FeII	10.94	-0.94	-3.90
6164.93	TiII	8.12	-0.40	-5.65
6165.89	FeII	9.74	-2.30	-5.65

Table 4: *Line parameters for calculation of synthetic spectra (continued)*

λ,Å	Ion	ε eV	log gf	logN
6213.13	Fe I	2.22	-2.46	-4.40
6214.95	FeII	11.11	-0.37	-4.40
6217.28	NeI	16.62	-1.14	-2.94
6262.29	LaII	0.40	-1.24	-10.6
6264.21	FeII	9.76	-1.55	-3.90
6264.36	FeII	11.27	0.05	-3.90
6265.01	CrII	11.08	-2.78	-4.68
6265.13	FeI	2.18	-2.25	-3.90
6265.32	CrI	4.41	-3.59	-4.68
6265.90	VII	6.07	-2.52	-7.23
6266.50	NeI	16.71	-0.53	-2.74
6269.62	FeII	13.78	0.36	-3.90
6269.97	FeII	3.24	-4.96	-3.90
6288.74	FeII	10.91	-0.75	-3.90
6289.73	FeII	11.27	-0.36	-3.90
6291.83	FeII	10.93	0.30	-3.90
6293.30	FeII	11.02	-1.00	-3.90
6293.74	NeI	18.69	-1.77	-2.76
6301.50	FeI	3.65	-0.75	-4.10
6302.49	FeI	3.69	-1.20	-4.10
6304.79	NeI	16.67	-0.90	-2.76
6305.30	FeII	6.22	-2.04	-4.00
6305.43	SII	14.17	-0.08	-4.44
6305.48	SII	14.17	-0.09	-4.44
6113.69	NeI	18.69	-1.91	-2.76
6328.01	FeII	11.29	-1.29	-4.30
6328.16	NeI	18.70	-1.42	-2.74
6328.50	FeII	10.99	-0.25	-4.30
6328.88	FeII	11.29	-1.363	-4.30
6330.40	CrII	11.14	-0.69	-4.68
6330.89	NeI	18.61	-1.76	-2.74
6330.91	FeI	11.45	-2.26	-4.30
6331.95	FeII	6.22	-1.98	-4.30
6332.86	SeII	7.43	-1.74	-7.61
6333.23	CrII	11.08	-0.23	-4.68
6334.08	TiII	8.24	-2.08	-5.65
6334.43	NeI	16.62	-0.31	-2.74
6335.70	AlII	13.65	-0.56	-5.55
6335.71	CI	8.77	-2.37	-3.32
6335.74	CrII	13.09	-0.99	-4.68
6351.86	NeI	18.71	-2.04	-2.64

Table 4: *Line parameters for calculation of synthetic spectra (continued)*

λ,Å	Ion	ε eV	log gf	logN
6382.99	NeI	16.67	-0.26	-2.74
6397.36	SII	14.16	-1.02	-3.94
6397.37	VII	4.78	-1.02	-3.58
6397.60	NiII	14.88	-3.51	-6.17
6397.70	NiII	12.91	0.98	-6.17
6397.86	CrII	11.14	-1.14	-4.78
6398.01	SII	14.15	-1.01	-3.94
6398.12	NiII	14.87	-1.56	-6.17
6398.25	NiII	14.68	-0.62	-6.17
6398.33	CrII	11.04	-3.70	-4.78
6398.40	NI	11.75	-3.43	-1.99
6398.43	CrII	11.63	-3.48	-4.78
6398.56	CrII	9.30	-4.44	-4.78
6399.17	CrII	13.04	-0.77	-4.78
6399.28	CrII	11.14	-0.61	-4.78
6399.62	FeII	8.61	-2.64	-3.90
6399.78	FeII	11.09	-1.20	-3.90
6400.45	FeII	11.05	-2.36	-3.90
6400.49	FeII	6.81	-3.06	-3.90
6400.97	CrII	11.63	-3.29	-4.78
6401.08	NeI	18.73	-1.65	-2.66
6401.93	NiII	14.99	0.75	-6.17
6402.25	NeI	16.62	0.34	-2.76
6402.36	NI	11.75	-1.97	-1.99
6403.71	SI	7.87	-1.43	-3.94
6404.12	FeII	7.14	-3.01	-3.90
6404.43	TiII	4.11	-1.04	-5.35
6404.87	FeII	7.14	-3.23	-3.90
6421.71	NeI	18.72	-1.97	-2.76
6502.85	VII	9.34	-0.34	-7.23
6503.40	PII	10.91	-0.01	-6.12
6503.62	FeII	9.58	-2.60	-3.90
6505.03	FeII	6.22	-3.06	-3.90
6506.02	FeII	9.78	-2.81	-3.90
6506.30	NI	11.76	-3.37	-2.59
6506.33	FeII	5.59	-3.11	-3.90
6506.53	NeI	16.67	0.01	-2.76
6507.98	PII	10.89	-0.18	-6.12
6508.17	CrII	11.14	-0.71	-4.68
6529.73	NI	11.75	-2.89	-1.89
6530.61	SII	13.66	-1.33	-4.56
6531.15	FeII	11.05	-0.42	-4.30
6531.24	ScII	7.44	-1.35	-7.91

Table 4: *Line parameters for calculation of synthetic spectra (continued)*

λ,Å	Ion	ε eV	log gf	logN
6531.76	FeII	9.74	-1.44	-4.30
6532.55	NII	23.24	-0.89	-2.29
6532.88	NeI	16.71	-0.70	-3.06
6534.24	CrII	13.15	-0.33	-4.48
6534.47	FeII	11.08	-0.45	-4.30
6598.95	NeI	16.85	-0.35	-2.66
6602.91	NeI	18.69	-1.76	-2.85
6673.74	PI	7.96	-1.45	-4.12
6674.11	CI	8.85	-2.25	-2.02
6676.34	CrII	11.49	-0.55	-4.08
6677.30	FeII	7.27	-1.59	-4.20
6678.15	HeI	21.22	0.33	-0.04
6678.28	NeI	16.85	-0.40	-3.06
6678.33	NeI	18.70	-1.53	-2.76
6678.83	FeII	10.93	-0.45	-4.20
6679.62	NI	12.12	-2.51	-2.19
6679.75	FeII	10.91	-0.47	-4.20
6717.04	NeI	16.85	-0.31	-2.90
6926.67	NI	11.84	-1.47	-2.19
6927.85	FeII	11.26	0.33	-4.20
6927.96	FeII	11.21	-1.88	-4.20
6928.55	FeII	11.67	-2.29	-4.20
6929.47	NeI	16.85	0.03	-2.66
6929.63	FeII	11.24	-1.97	-4.20
6929.72	CI	8.64	-2.26	-2.62
6931.09	CrII	11.53	-1.86	-4.48
6931.35	FeII	10.40	-2.98	-4.20
6932.00	FeII	11.31	0.23	-4.20
7030.18	FeII	11.44	-2.68	-3.90
7030.28	FeII	11.29	-0.63	-3.90
7030.78	FeII	11.49	-2.94	-3.90
7031.44	FeI	4.99	-2.17	-3.90
7031.59	FeII	11.22	-2.54	-3.90
7031.61	FeII	11.14	-3.24	-3.90
7032.21	VII	9.42	-3.24	-6.53
7032.41	NeI	16.62	-0.25	-2.64
7033.75	FeII	11.26	-1.45	-3.90
7173.94	NeI	16.85	-1.31	-2.94
7240.11	CI	8.64	-1.46	-2.32
7242.43	NeI	19.69	-4.65	-2.74

Table 4: *Line parameters for calculation of synthetic spectra (continued)*

λ,Å	Ion	ε eV	log gf	logN
7242.50	SI	8.04	-1.30	-3.94
7245.17	NeI	16.67	-0.60	-2.60
7304.82	NeI	18.96	-2.17	-2.74
7438.90	NeI	16.71	-1.15	-2.64
7485.03	HeI	22.92	-3.93	-0.04
7485.18	NI	12.01	-1.57	-2.29
7485.26	FeII	11.29	-1.52	-4.20
7485.89	TiII	8.47	-1.24	-5.90
7488.87	NeI	18.38	-0.30	-2.96
7490.32	SiII	14.78	-1.20	-3.30
7493.22	ScII	8.26	0.13	-8.11
7494.98	CrII	11.63	-0.33	-4.68

NeI λ 7242.43. The lines of the stellar spectrum are lost against the background of the atmosphere lines. The neon abundance estimate is not very reliable: $\log(N(Ne)/\Sigma N_i) = -2.74$.

NeI λ 7488.87. The wings of the observed contour are broader than the theoretical ones by 0.2 Å for the line depth of 0.4. The neon abundance: $\log(N(Ne)/\Sigma N_i) = -2.94$.

For the rest of the calculated lines the coincidence is the same as shown in Fig. 3.

When calculating neon lines, the Stark broadening parameters calculated by Griem (1969) were employed. A comparison of the theoretical calculations with the observed spectra, the results of which are given in the last column of Table 4, gives an average value of neon abundance in the atmosphere of the υ Sgr main component: $\log(N(Ne)/\Sigma N_i) = -2.78 \pm 0.13$, which within the errors coincides with the values derived from the line equivalent widths. The average over these values is $\log(N(Ne)/\Sigma N_i) = -2.76 \pm 0.16$.

6. Conclusions

The analysis made in the paper yields a reliable enough value of neon abundance in the atmosphere of the main component of υ Sgr: $\log(N(Ne)/\Sigma N_i) = -2.76 \pm 0.16$. Besides, the calculation results given in Table 4 allow us to estimate also the abundances of some other elements. Table 5 presents the abundances of light elements, which we have redetermined for the atmosphere of υ Sgr as compared with the solar ones.

It should be noted that the value of neon abundance presented here (amounting to 1 % in mass) has been obtained with the turbulent velocity 12 km/s. If the value $V_t = 7.5$ km/s, found from iron lines, is used in the calculations, then the neon abundance will be by 0.6 dex higher, which yields in the number of

Table 5: *Light element abundances in the atmosphere of υ Sgr and the Sun*

Element	From the number of atoms $\log(N_k/\Sigma N_i)$		From the mass $\log(\mu_k \cdot N_k/\Sigma(\mu_i \cdot N_i))$	
	υ Sgr	Sun	υ Sgr	Sun
H	-3.40	-0.05	-4.00	-0.15
He	-0.01	-1.00	-0.03	-0.58
C	-2.31	-3.50	-1.85	-2.40
N	-2.15	-4.12	-1.64	-3.00
O	-3.41	-3.28	-2.70	-2.15
Ne	-2.76	-3.90	-2.05	-2.70

atoms $\log N(Ne)/\Sigma N_i = -2.26$, about 3% in mass. So, neon is really one of the most abundant elements (after helium, nitrogen and carbon) in the atmosphere of the star under study.

There is no doubt that the nature of neon overabundance is related directly to the nuclear evolution of the star in its interior. Most likely, here we observe neon formed as a result of reactions of helium with carbon and oxygen

$$^{12}C(\alpha,\gamma)^{16}O(\alpha,\gamma)^{20}Ne$$

in the star's core and then swept to the layers observable now owing to loss of the envelope. In this case, we must assume that during the period of helium burning in the core of υ Sgr in the triple α-process, carbon is rapidly converted to oxygen and the latter is converted to neon. At the same time, another neon isotope may possibly form in a nuclear chain with nitrogen

$$^{14}N(\alpha,\gamma)^{18}F(\beta^+,\nu)^{18}O(\alpha,\gamma)^{22}Ne.$$

Taking into account that a high nitrogen abundance (second after helium abundance) is observed in υ Sgr, we may assume that neon is generated simultaneously with nitrogen generation. Such a situation is possible within the framework of our proposed model of evolution of υ Sgr chemical composition (Leushin et al., 1998). The mixing between the zones of hydrogen and helium burning, mentioned in that paper, causes carbon, generated in the zone of helium burning, after getting into the layer source of hydrogen to convert into nitrogen. Then the matter enriched with nitrogen, when getting into the zone of helium burning, increases the amount of neon, which is then swept again to the upper layers. Thus, simultaneous enrichment in nitrogen and neon is provided.

Acknowledgements. The author is grateful to F. Musaev and E. Kajsina for obtaining and primary processing of υ Sgr spectra. This work is supported by the grant of RFBR No.00-02-16213-a.

References

Griem H.R., 1974, Spectral line broadening of plasma, Acad. Press, NY and London

Kasabov G.A., Eliseev V.V., 1973, Spectroscopic tables for low-temperature plasma (in Russian), Moscow, Atomizdat

Kravtsov V.V., Leushin V.V., 1981, Spectrophotometric analysis of the atmosphere of the binary system υ Sgr bright component (in Russian), Dep. No.99–82

Leushin V.V., 1995, Astron. Zh., **72**, 543

Leushin V.V. Snezhko L.I., Chuvenkov V.V., 1997, Bull. Spec. Astrophys. Obs., **43**, 55

Leushin V.V. Snezhko L.I., Chuvenkov V.V., 1998, Pis'ma Astron. Zh., **24**, 45

Leushin V.V., Topilskaya G.P., 1985, Astrofizika, **22**, 121

Leushin V.V., Topilskaya G.P., 1986, Astrofizika, **25**, 103

Leushin V.V., Topilskaya G.P., 1987, Astrofizika, **26**, 195

Lyubimkov L.S., Samedov Z.A., 1990, Astrofizika, **32**, 49

Musaev F.A., 1993, Pis'ma Astron. Zh., **19**, 776

Ryabchikova T.A., Piskunov N.E., Stempels H.C., Kupka F., Weiss W.W., 1999, Physika Scripta Peoc. of ASOS6, (in press)